

Supporting Information

Quaternary FeCoNiMn-based nanocarbon electrocatalysts for bifunctional oxygen reduction and evolution: promotional role of Mn doping in stabilizing carbon

Shiva Gupta,[†] Shuai Zhao,[‡] Xiao Xia Wang,[†] Sooyeon Hwang,[§] Stavros Karakalos,[¶] Surya V. Devaguptapu,[†] Shreya Mukherjee,[†] Dong Su,[§] Hui Xu,[‡] and Gang Wu^{†,*}

[†] Department of Chemical and Biological Engineering, University at Buffalo, The State University of New York, Buffalo, NY 14260, United States

[‡] Giner Inc., Newton, MA 02466, United States

[§] Center for Functional Nanomaterials, Brookhaven National Laboratory, Upton, NY 11973, United States

[¶] Department of Chemical Engineering, University of South Carolina, Columbia, SC 29208, United States

Corresponding author. E-mail address: gangwu@buffalo.edu (G. Wu)

Figure S1 to S10

Table S1 to S5

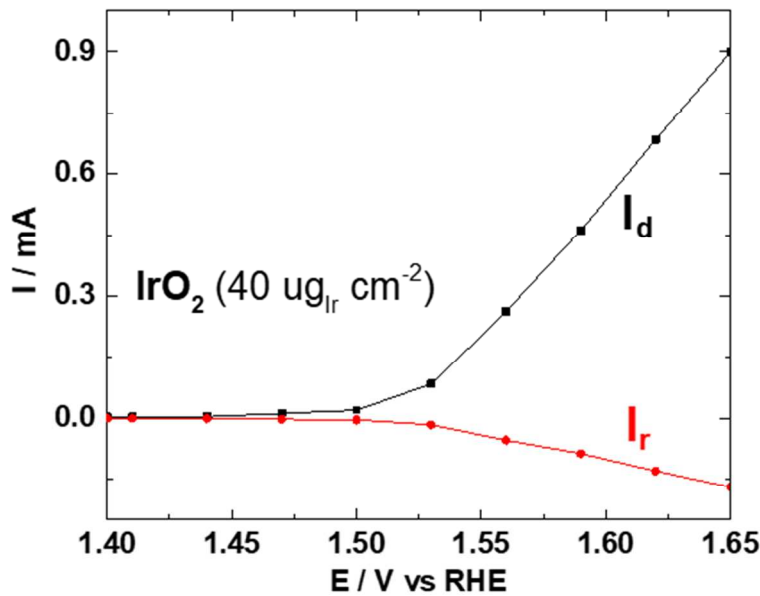


Figure S1. RRDE steady-state polarization plots conducted in N_2 purged 0.1 M NaOH for 30 min and then blanketed during the OER experiment on commercial IrO_2 . I_d and I_r corresponds to disk and ring current, respectively. The collection efficiency was calculated from this data, which was then used to calibrate ring current for NC-FeCoNiMn_4 as shown in Figure 1d.

In order to calculate collection efficiency of ring of RRDE, commercial IrO_2 catalyst was used. Oxidation current of IrO_2 should be nearly 100 % Faradaic efficiency¹ and exclusive to carbon oxidation during OER. The collection efficiency (N) was calculated to for each data point (between 1.4 V and 1.65 V) as follows:

$$N = I_r/I_d$$

where I_d denotes disk current, I_r denotes ring current and N denotes collection efficiency of the RRDE. The collection efficiency was determined to be 0.19 with 1 % error between different data points. Thus, the same collection efficiency was used to calibrate ring current for NC-FeCoNiMn_4 as shown in Figure 1d.

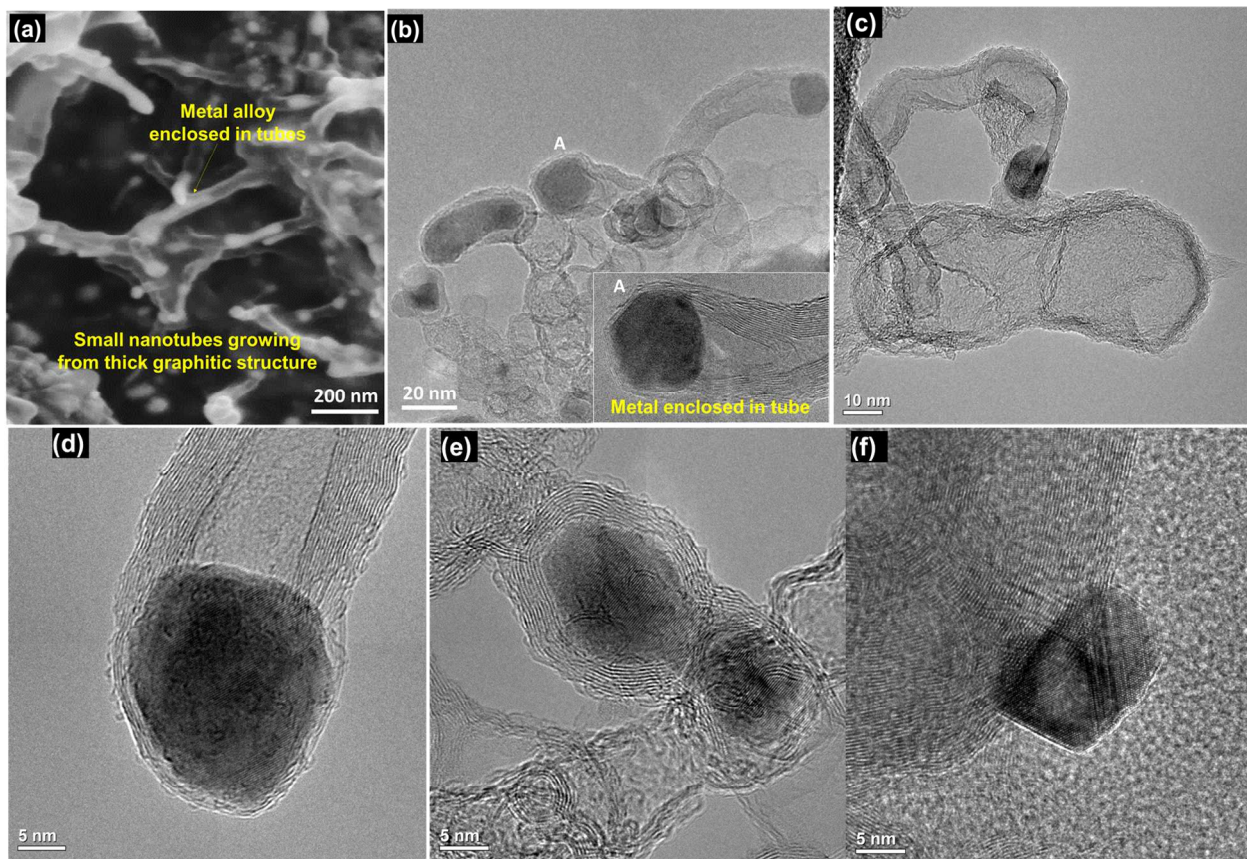


Figure S2. Typical SEM (a) and HR-TEM (b-f) images for the best performing NC-FeCoNiMn₄ catalyst

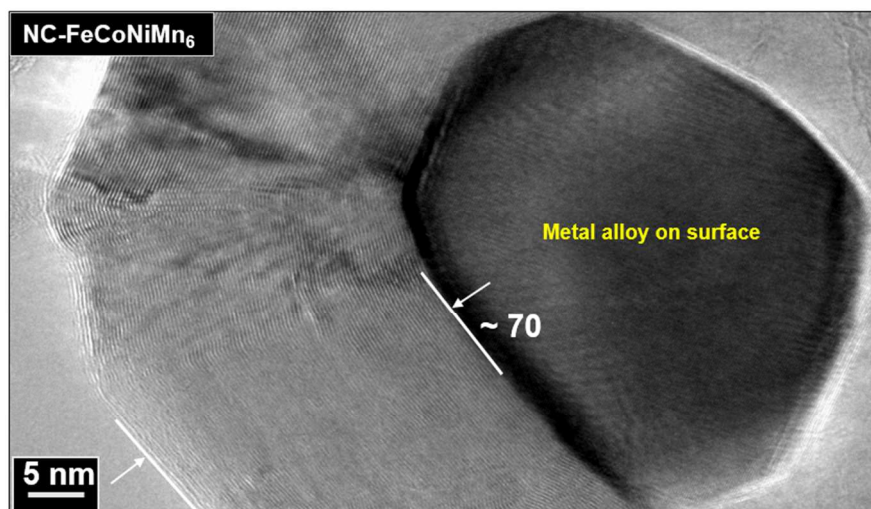


Figure S3. HR-TEM images for Mn dominant NC-FeCoNiMn₆. (scale bar is 5 nm; numbers of graphitic layers (G_#) are labeled).

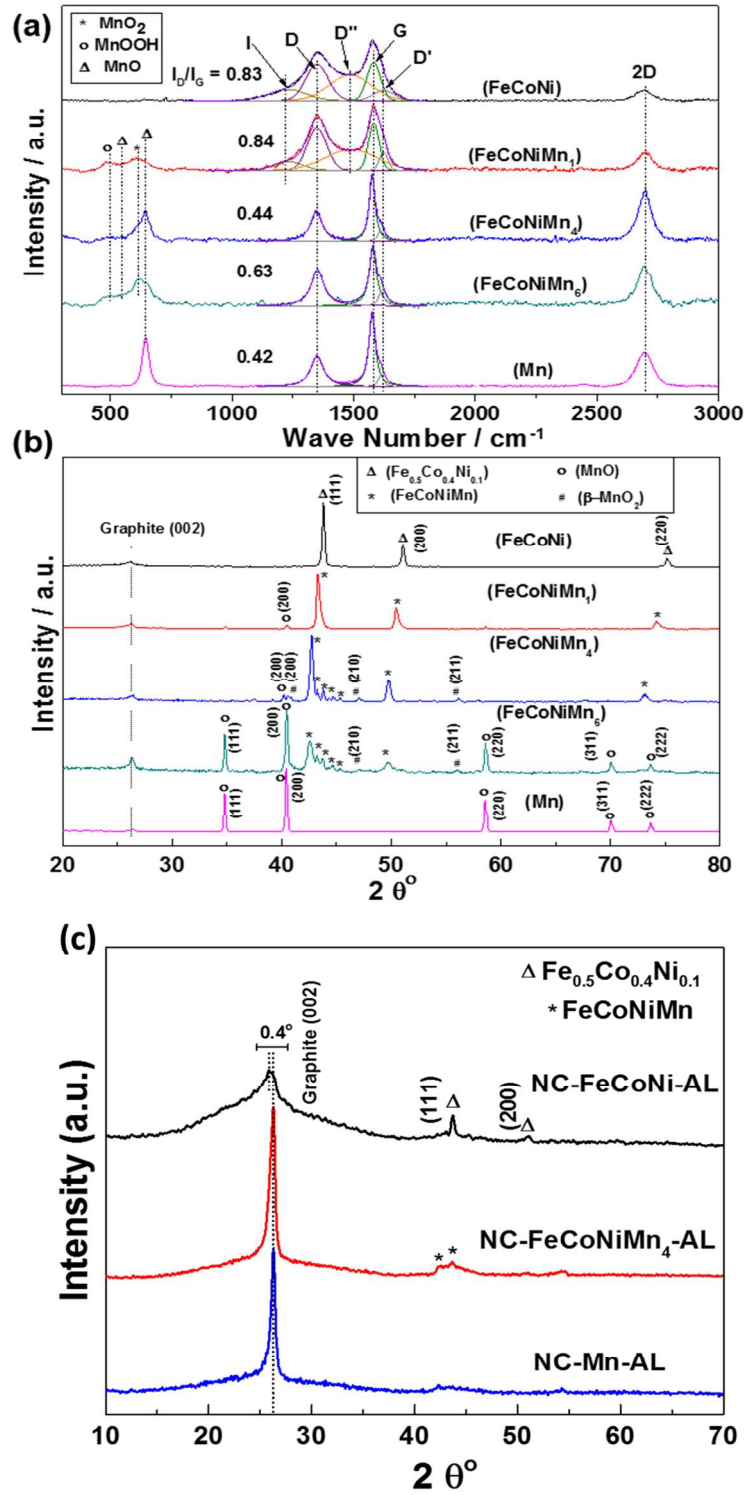


Figure S4. (a) Raman spectra and (b) X-ray diffraction patterns for various catalysts including NC-FeCoNi, NC-Mn, and NC-FeCoNiMn_x ($x=1, 4$ and 6). (c) XRD patterns of the acid leached catalyst samples including NC-FeCoNi-AL (black), NC-FeCoNiMn₄-AL (red), and NC-Mn-AL (blue).

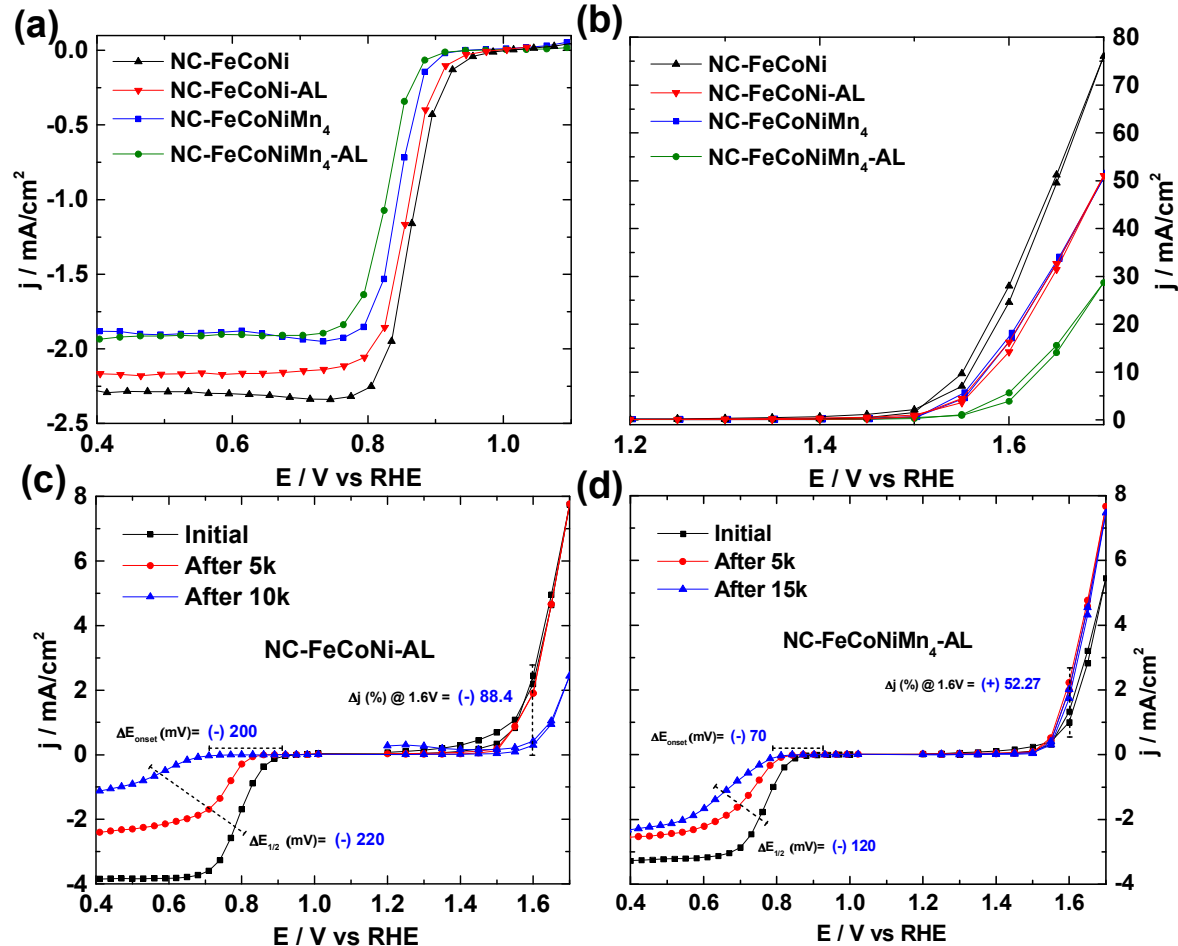


Figure S5. Steady-state polarization plots of various catalysts at 25 °C for (a) the ORR at 900 rpm in O₂ saturated 1.0 M NaOH and (b) the OER at 1600 rpm in 1.0 M NaOH. Potential cycling stability (between 0-1.9 V vs. RHE using 500 mV s⁻¹) in O₂ saturated 0.1 M NaOH for (c) NC-FeCoNi-AL (after acidic leaching treatment) and (d) NC-FeCoNiMn₄-AL.

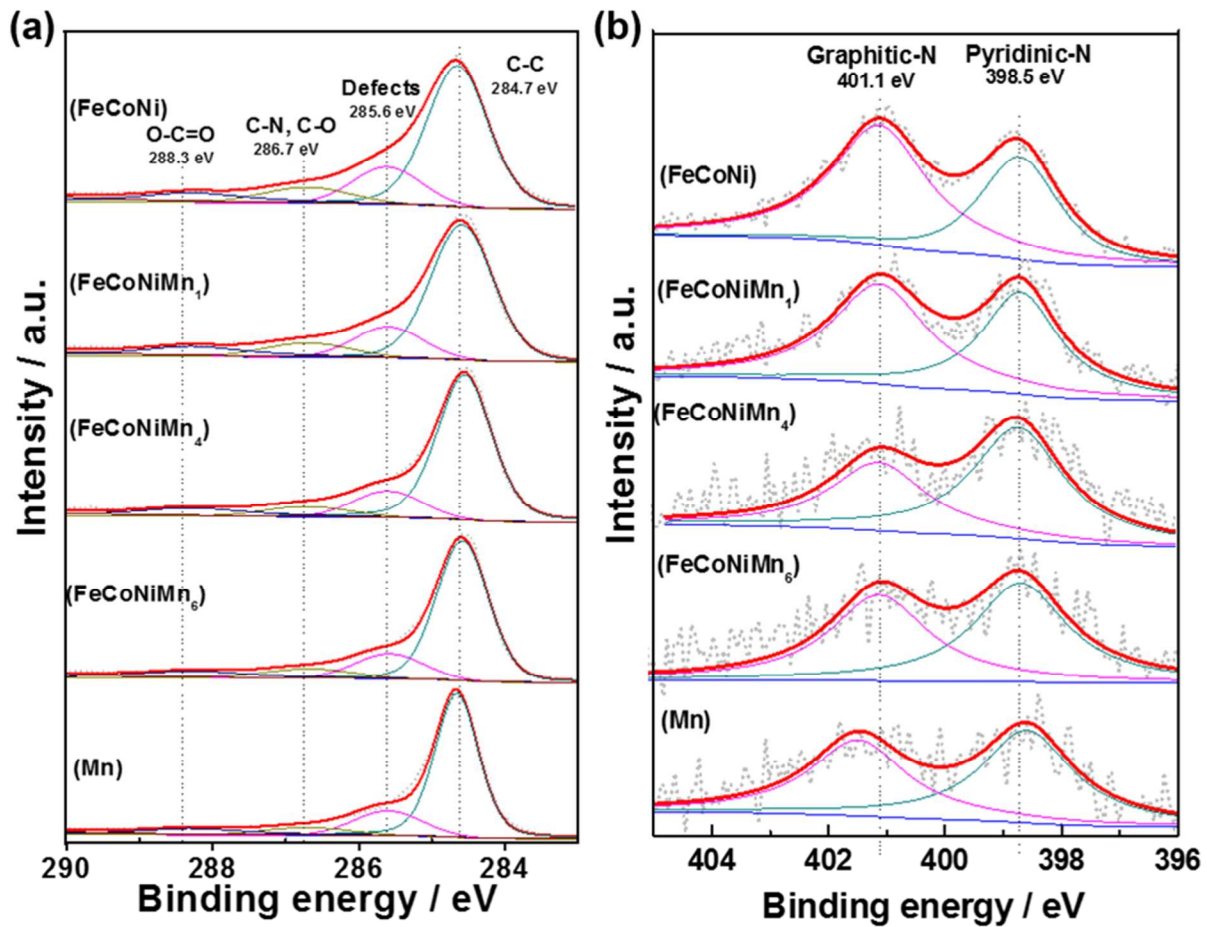


Figure S6. High-resolution XPS (a) C 1s and (b) N 1s for various catalysts.

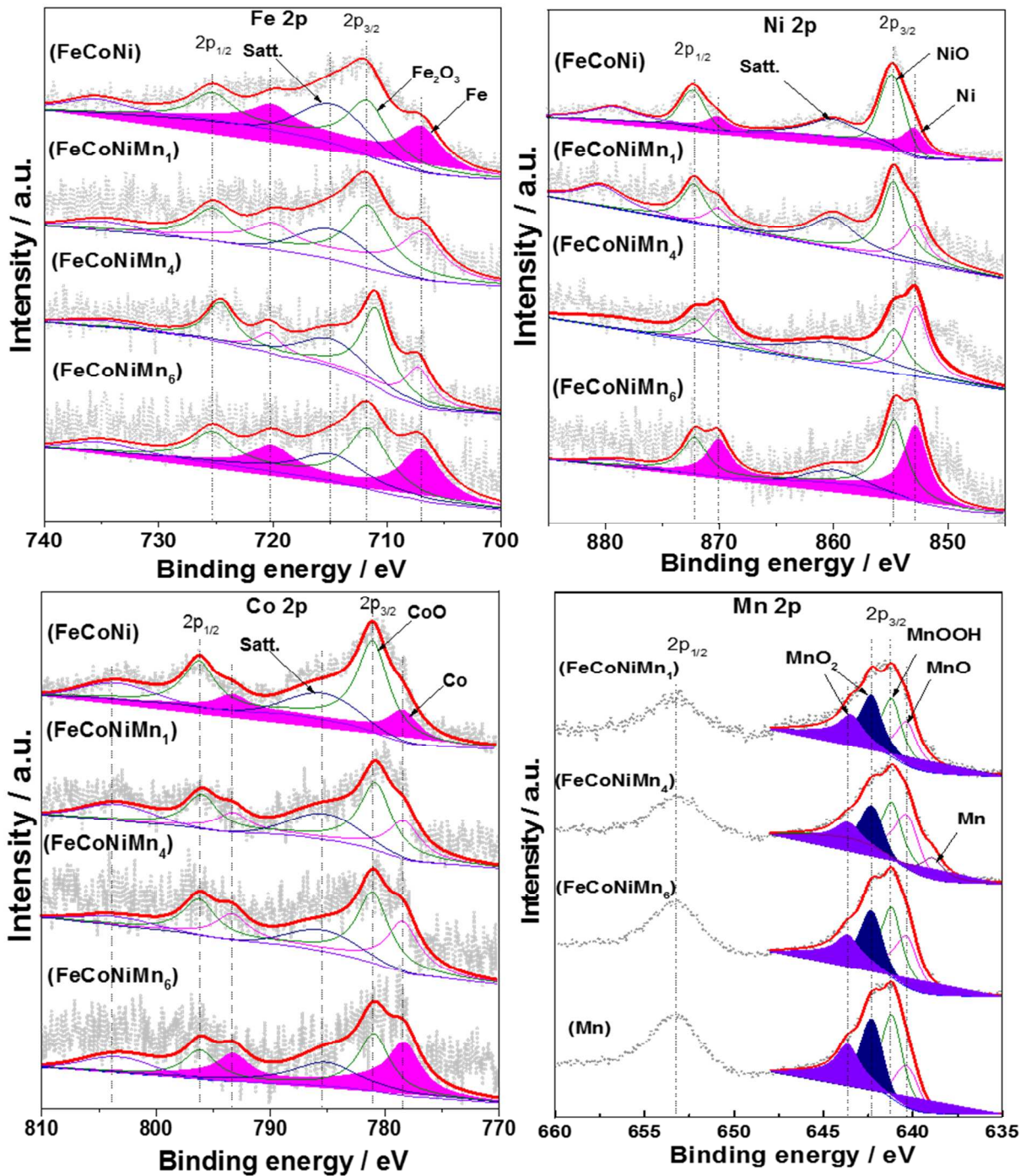


Figure S7. High-resolution XPS for Fe, Ni, Co, and Mn for various catalysts.

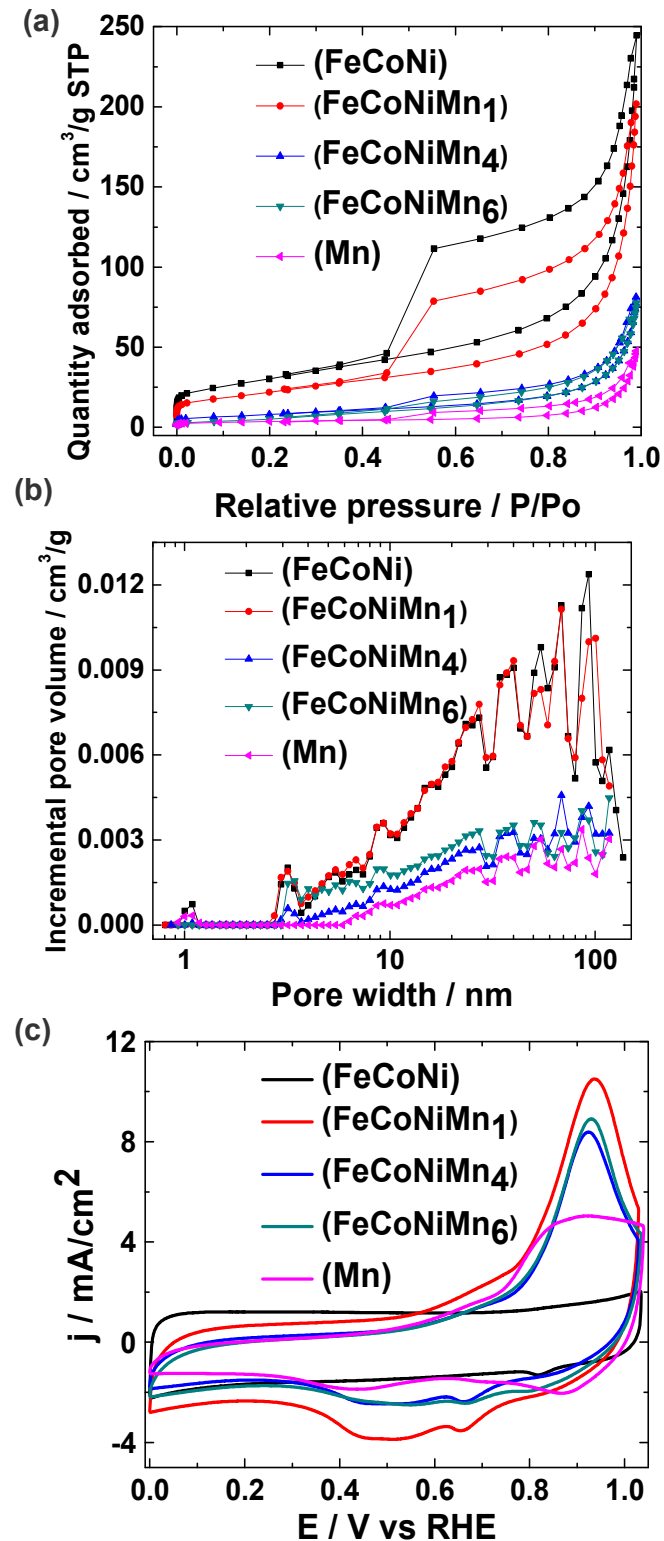


Figure S8. Brunauer–Emmett–Teller surface area analysis to determine (a) N₂ adsorption–desorption isotherms and (b) pore size distribution for catalysts. (c) Cyclic voltammetry recorded in N₂ purged 1.0 M NaOH at a scan rate of 50 mV s⁻¹ and 25 °C. These polarization plots were used to determine electrochemically active surface area.

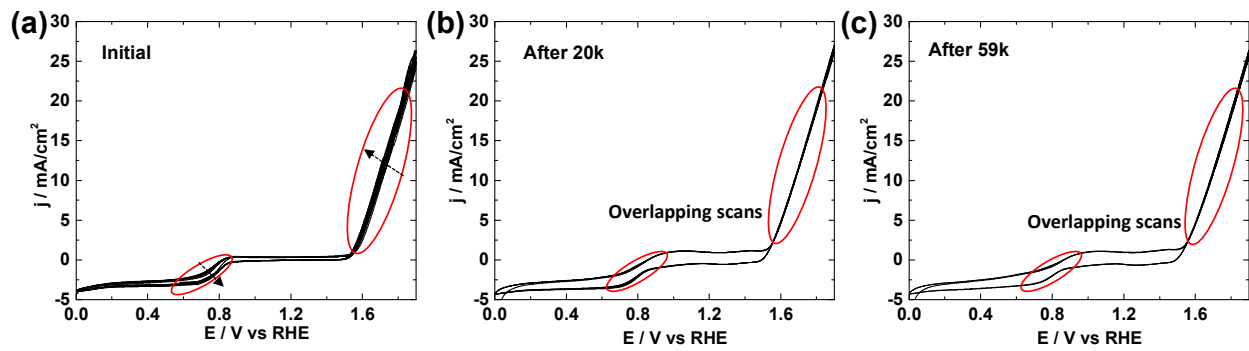


Figure S9. Cyclic voltammetry recorded between 0-1.9 V vs. RHE at a scan rate of 500 mV/s in O₂ saturated 0.1 M NaOH for NC-FeCoNiMn₄. Each figure shows 25 consecutive cycles at different stages.

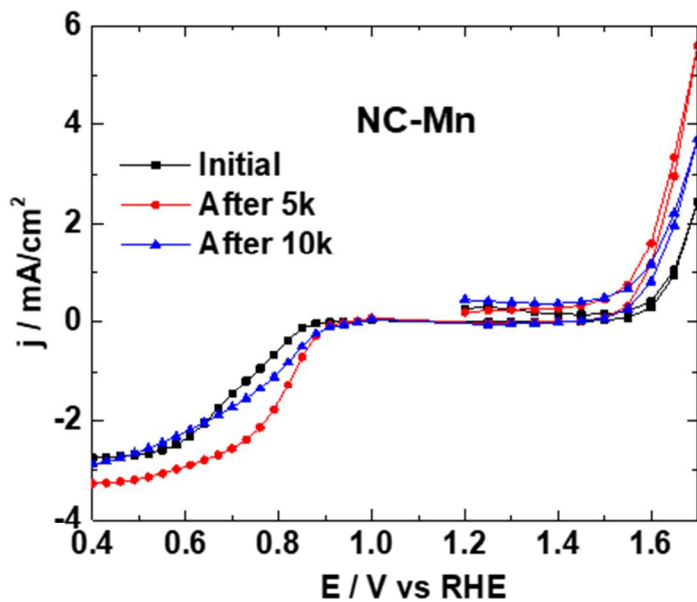


Figure S10. AST stability by using potential cycling (0-1.9 V, 500 mVs⁻¹) in O₂ saturated 0.1 M NaOH, 25°C for NC-Mn catalyst. It eventually exhibited degradation during the long-term AST.

Table S1. ORR E_{onset} , ORR $E_{1/2}$, OER E_{onset} and OER $j@1.6$ V calculated from steady state polarization plots.

Catalysts	ORR E_{onset} (V vs RHE, $j = -0.01$ mA cm $^{-2}$)	ORR $E_{1/2}$ (V vs RHE)	OER E_{onset} (V vs RHE, $j = 1.0$ mA cm $^{-2}$)	$j_{OER} @ 1.6$ V (mA cm $^{-2}$)
NC-FeCoNi	0.95	0.87	1.47	28.0
NC-FeCoNiMn1	0.94	0.86	1.50	17.7
NC-FeCoNiMn4	0.94	0.85	1.50	18.2
NC-FeCoNiMn6	0.92	0.83	1.51	9.2
NC-Mn	0.90	0.82	1.63	0.4
Pt/C	0.98	0.90	n/a	n/a
IrO ₂	n/a	n/a	1.52	7.4

Table S2. A comparison of studied nanocarbon composite catalysts and other ORR/OER reported catalysts in terms of their activity in alkaline electrolyte.

PGM-free bifunctional catalysts	E -ORR (V vs. RHE, $j = -1$ mA cm $^{-2}$)	E -OER (V vs. RHE, $j = 10$ mA cm $^{-2}$)	Electrolyte	Catalyst's loading (mg cm $^{-2}$)	Reference
NC-FeCoNiMn ₄	0.86	1.57	1.0 M NaOH	0.80	This work
NPMC-1000	0.86	n/a	0.1 M KOH	0.45	²
Zn-Co-S NN/CFP	0.74	1.55	1.0 M KOH	0.60	³
Co ₃ O ₄ /MnO ₂ -CNTs	0.92	1.74	0.1 M KOH	0.125	⁴
Co ₃ O ₄ /MnO ₂ -CNTs	0.82	n/a	0.1 M KOH	0.10	⁵
Ni/NiO/NiCo2O4/N-CNT-As	0.79	1.46	0.1 M KOH (ORR) & 1.0 M KOH	0.24	⁶
NiCo2O4-CNTs-400	0.83	1.66	0.1 M KOH	0.10	⁷
Co ₃ O ₄ /NBGHSS	0.88	1.72	0.1 M KOH	n/a	⁸
Co/CoO@Co-N-C-800	-0.17*	0.62*	0.1 M KOH	n/a	⁹
NiFeO@MnO _x (1:0.8)	0.82	1.65	0.1 M KOH	0.10	¹⁰
Co ₄ Mn ₁	0.96	1.57	0.1 M KOH	0.10 for ORR and 1.0 or OER	¹¹
LMCO/NCNT	-0.22**	0.75	n/a	0.41	¹²
NCNT/Co _x Mn _{1-x} O	0.83	1.57	1.0 M KOH	0.21	¹³
NCNT/CoO-NiO-NiCo	0.82	1.49	0.1 M KOH (ORR) & 1.0 M	0.21	¹⁴

			KOH (OER)		
NiCo ₂ S ₄ /N-CNT	0.81	1.6	0.1 M KOH	0.25	¹⁵
ZnCo ₂ O ₄ /N-CNT	0.85	1.64	0.1 M KOH	0.20	¹⁶

Table S3. Quantification of surface atomic composition of the studied nanocarbon composite catalysts determined by using XPS.

Catalysts	Surface atomic composition (at%)						
	C	N	O	Fe	Co	Ni	Mn
NC-FeCoNi	95.5	2	1.8	0.2	0.2	0.3	-
NC-FeCoNiMn ₁	96.1	1.4	1.8	0.1	0.1	0.1	0.4
NC-FeCoNiMn ₄	93.5	1	4.2	0.2	0.1	0.2	0.8
NC-FeCoNiMn ₆	93.8	0.7	4.3	0.1	0.1	0.1	0.9
NC-Mn	93.4	0.7	4.8	-	-	-	1.1

Table S4. Quantification of bulk elemental composition for the studied nanocarbon composite catalysts using Energy dispersive X-ray spectroscopy (EDS) couple with SEM.

Catalysts	EDS - Bulk atomic composition (wt%)						
	C	N	O	Fe	Co	Ni	Mn
NC-FeCoNi	86.4	2.3	4.1	2.7	2.4	2.1	-
NC-FeCoNiMn ₁	81.4	1.3	4.3	3.8	3.1	2.9	3.2
NC-FeCoNiMn ₄	80.2	1.1	4.4	2.2	2	1.7	8.4
NC-FeCoNiMn ₆	80.3	n/a*	4.8	2	1.6	1.5	8.9
NC-Mn	80.7	n/a*	6.3	-	-	-	12.3

*below the detection limit of EDS

Table S5. BET specific surface area, pore volume, average pore size and electrochemically accessible surface areas (EASA) of the studied nanocarbon composite catalysts.

Catalyst	Total pore vol.(cm ³ /g)	Ave. pore size (nm)	Specific surf. Area (m ² /g)	EASA (1.0 M NaOH) (m ² /g)
NC-FeCoNi	0.33	12.61	107.57	98.67
NC-FeCoNiMn₁	0.27	14.21	78.36	60.63
NC-FeCoNiMn₄	0.11	15.60	28.77	21.23
NC-FeCoNiMn₆	0.10	15.93	21.50	11.05
NC-Mn	0.06	22.09	12.45	11.37

References

- (1) Nakagawa, T.; Bjorge, N. S.; Murray, R. W., *J. Am. Chem. Soc.* **2009**, 131, 15578-15579.
- (2) Zhang, J.; Zhao, Z.; Xia, Z.; Dai, L., *Nat. Nanotechnol.* **2015**, 10, 444-452.
- (3) Wu, X.; Han, X.; Ma, X.; Zhang, W.; Deng, Y.; Zhong, C.; Hu, W., *ACS Appl. Mater. Interfaces* **2017**, 9, 12574-12583.
- (4) Li, X.; Xu, N.; Li, H.; Wang, M.; Zhang, L.; Qiao, J., *Green Energy Environ.* **2017**, 2, 316-328.
- (5) Xu, N.; Liu, Y.; Zhang, X.; Li, X.; Li, A.; Qiao, J.; Zhang, J., *Sci. Rep.* **2016**, 6, 33590.
- (6) Ma, N.; Jia, Y.; Yang, X.; She, X.; Zhang, L.; Peng, Z.; Yao, X.; Yang, D., *J. Mater. Chem. A* **2016**, 4, 6376-6384.
- (7) Ma, C.; Xu, N.; Qiao, J.; Jian, S.; Zhang, J., *Int. J. Hydrogen Energy* **2016**, 41, 9211-9218.
- (8) Jiang, Z.; Jiang, Z.-J.; Maiyalagan, T.; Manthiram, A., *J. Mater. Chem. A* **2016**, 4, 5877-5889.
- (9) Zhang, X.; Liu, R.; Zang, Y.; Liu, G.; Wang, G.; Zhang, Y.; Zhang, H.; Zhao, H., *Chem. Commun.* **2016**, 52, 5946-5949.
- (10) Cheng, Y.; Dou, S.; Veder, J.-P.; Wang, S.; Saunders, M.; Jiang, S. P., *ACS Appl. Mater. Interfaces* **2017**, 9, 8121-8133.
- (11) Wang, Z.; Xiao, S.; An, Y.; Long, X.; Zheng, X.; Lu, X.; Tong, Y.; Yang, S., *ACS Appl. Mater. Interfaces* **2016**, 8, 13348-13359.
- (12) Lee, D. U.; Park, M. G.; Park, H. W.; Seo, M. H.; Ismayilov, V.; Ahmed, R.; Chen, Z., *Electrochem. Commun.* **2015**, 60, 38-41.
- (13) Liu, X.; Park, M.; Kim, M. G.; Gupta, S.; Wang, X.; Wu, G.; Cho, J., *Nano Energy* **2016**, 20, 315-325.
- (14) Liu, X.; Park, M.; Kim, M. G.; Gupta, S.; Wu, G.; Cho, J., *Angew. Chem. Int. Ed.* **2015**, 54, 9654-9658.
- (15) Han, X.; Wu, X.; Zhong, C.; Deng, Y.; Zhao, N.; Hu, W., *Nano Energy* **2017**, 31, 541-550.
- (16) Liu, Z.-Q.; Cheng, H.; Li, N.; Ma, T. Y.; Su, Y.-Z., *Adv. Mater.* **2016**, 28, 3777-3784.